materials

MDPI

Article

Comparison of Cinchona Catalysts Containing Ethyl or Vinyl or Ethynyl Group at Their Quinuclidine Ring

Sándor Nagy [1], Zsuzsanna Fehér [1], Gergő Dargó [1,2], Júlia Barabás [3], Zsófia Garádi [3], Béla Mátravölgyi [1], Péter Kisszékelyi [1], Gyula Dargó [1], Péter Huszthy [1], Tibor Höltzl [3,4], György Tibor Balogh [2,5,*] and József Kupai [1,*]

1 Department of Organic Chemistry & Technology, Budapest University of Technology & Economics, Szent Gellért tér 4, H-1111 Budapest, Hungary; nagy.sandor@mail.bme.hu (S.N.); zsuzsi516@gmail.com (Z.F.); dageri15@gmail.com (G.D.); bmatravolgyi@mail.bme.hu (B.M.); pkisszekelyi@mail.bme.hu (P.K.); huszthy@mail.bme.hu (P.H.)
2 Chemical Department, Chemical Works of Gedeon Richter Plc., P.O. Box 27, H-1103 Budapest, Hungary; gytbalogh@mail.bme.hu
3 Department of Inorganic & Analytical Chemistry, Budapest University of Technology & Economics, Szent Gellért tér 4, H-1111 Budapest, Hungary; julia.barabas@mail.bme.hu (J.B.); garadi.zsofia@egis.hu (Z.G.); tibor.holtzl@furukawaelectric.com (T.H.)
4 Furukawa Electric Institute of Technology, Késmárk utca 28/A, H-1158 Budapest, Hungary
5 Department of Chemical & Environmental Process Engineering, Budapest University of Technology and Economics, Műegyetem rkp. 3, H-1111 Budapest, Hungary
* Correspondence: jkupai@mail.bme.hu (J.K.); gytbalogh@mail.bme.hu (G.T.B.); Tel.: +36-1-463-2229 (J.K.); +36-1-463-2174 (G.T.B.)

Received: 22 August 2019; Accepted: 12 September 2019; Published: 18 September 2019

Abstract: Numerous cinchona organocatalysts with different substituents at their quinuclidine unit have been described and tested, but the effect of those saturation has not been examined before. This work presents the synthesis of four widely used cinchona-based organocatalyst classes (hydroxy, amino, squaramide, and thiourea) with different saturation on the quinuclidine unit (ethyl, vinyl, ethynyl) started from quinine, the most easily available cinchona derivative. Big differences were found in basicity of the quinuclidine unit by measuring the pK_a values of twelve catalysts in six solvents. The effect of differences was examined by testing the catalysts in Michael addition reaction of pentane-2,4-dione to *trans*-β-nitrostyrene. The 1.6–1.7 pK_a deviation in basicity of the quinuclidine unit did not result in significant differences in yields and enantiomeric excesses. Quantum chemical calculations confirmed that the ethyl, ethynyl, and vinyl substituents affect the acid-base properties of the cinchona-thiourea catalysts only slightly, and the most active neutral thione forms are the most stable tautomers in all cases. Due to the fact that cinchonas with differently saturated quinuclidine substituents have similar catalytic activity in asymmetric Michael addition application of quinine-based catalysts is recommended. Its vinyl group allows further modifications, for instance, recycling the catalyst by immobilization.

Keywords: organocatalysis; cinchona; squaramide; thiourea; pK_a; Michael addition

1. Introduction

Asymmetric syntheses went through explosive growth in the last decades [1–5]. After transition metal- and enzyme-based catalysis, the application of organocatalysis has gained ground in the field of asymmetric syntheses. The aim of enantioselective organocatalytic synthesis is to produce enantiopure compounds from achiral substrates facilitated by asymmetric organocatalysts. The importance of the

synthesis and application of enantiopure products lies in the fact that many industries are required to produce the appropriate enantiomer, for instance as drug or pesticide intermediates.

Within organocatalysis, bifunctional catalysts have become widespread. This bifunctionality means the capability to activate two components of a reaction simultaneously [6]. Cinchona moiety is one of the privileged chiral skeletons in asymmetric organocatalysis [7]. Its structure consists of two rigid rings, the aromatic quinoline, and the alicyclic quinuclidine rings. The tertiary amino group in the quinuclidine ring gives basic character for the molecule, hence this can activate/fix nucleophile or electrophile, and possessing a chiral skeleton, cinchona unit is also responsible for chiral induction.

There are many successful applications of cinchona-based organocatalysts in asymmetric reactions with high yields and enantiomeric excesses [8]. Such reactions include, but are not limited to, Morita–Baylis–Hillman reaction, Henry reaction, Diels–Alder reaction, and the most often examined, Michael addition. These reactions are used for the synthesis of drug intermediates, such as oseltamivir, baclofen, or prostaglandin E1 [9–11].

When bifunctional H-bond organocatalysts, such as cinchona-thioureas or squaramides were applied in Michael additions of 1,3-dioxo compounds to nitroalkenes, it was found [12–16] that the reaction can proceed by two mechanisms. In one of these mechanisms, the acidic NH groups (of thiourea or squaramide moieties) activate the enolate, while the protonated quinuclidine fixes the electrophile (Figure 1a). According to the other mechanism, the activation of substrates occurs on the opposite sites of catalysts (Figure 1b). Nevertheless, both mechanisms start with the deprotonation of the nucleophile by the basic N atom of the quinuclidine ring.

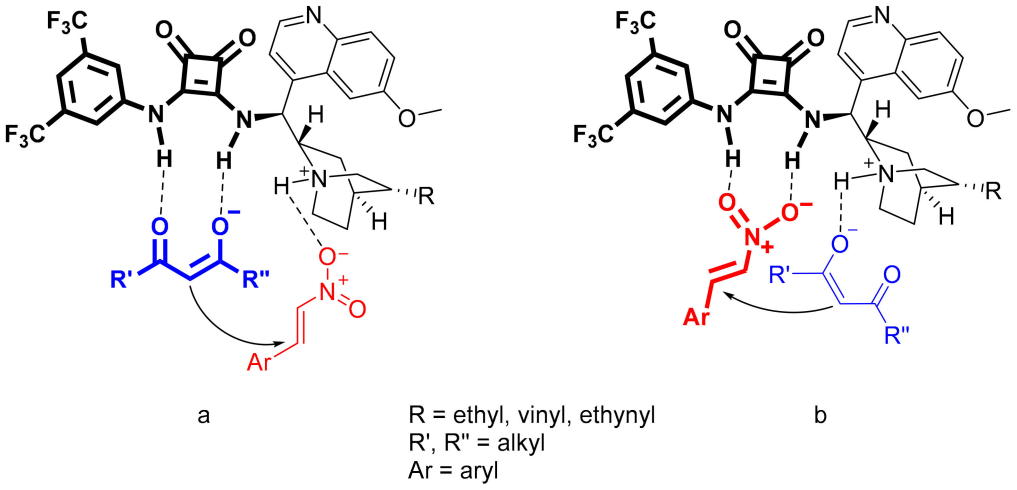

Figure 1. Two possible mechanisms (**a** and **b**) for Michael addition in the presence of bifunctional H-bond organocatalysts.

Based on these mechanisms, the basic N atom of the quinuclidine unit plays an important role in these reactions, which is related to its pK_a value. These cinchona-based organocatalysts are usually used with saturated or unsaturated substituent (ethyl, vinyl, ethynyl) on the quinuclidine ring, although the effect of that saturation has not been examined before. Vinyl or ethynyl group is often the target for further transformations (Figure 2) such as polymerization or immobilization [17–22]; however, several methods for modification are described in the literature in other positions of the cinchonas as well (C9 position, or modification after demethylation of quinoline) [23,24].

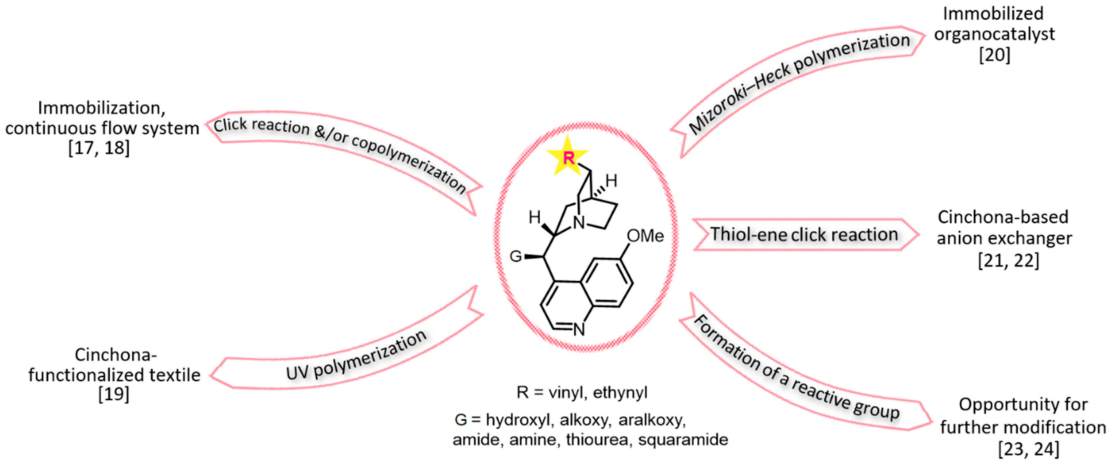

Figure 2. The possible direct modifications on the vinyl or ethynyl group of quinuclidine unit.

Herein we report the study of substituent influence on the basicity of cinchonas. We synthesized the appropriate hydroxyl, amino, thiourea, and squaramide cinchona derivatives with different saturation of the quinuclidine substituent. We measured the pK_a values of these derivatives in eight solvents and examined the catalytic activity of these twelve catalysts in Michael addition of pentane-2,4-dione to *trans*-β-nitrostyrene in seven solvents.

2. Results and Discussion

Since the strength of hydrogen bonding interactions plays an important role in H-bond organocatalysis [16,25–27], determination of pK_a values could help understanding the mechanisms and catalytic activity, therefore, it can contribute the design of more efficient catalytic systems. In cases when deprotonation and/or hydrogen bonding are able to promote reactions or could increase enantioselectivity, knowing the pK_a values of the corresponding groups is essential.

2.1. The pK_a Values of Conjugate Acid Forms of Quinuclidine

To get further insight into the H-bond organocatalytic behavior of the aforementioned twelve catalysts, the pK_a values of all four compound classes were measured in six different solvents by UV-spectrophotometric titrations (Pion Inc., Forest Row, UK) (Table 1 and Tables S1–S4). For better clarity, only those pK_a values are shown in Table 1 which were measured in water for the conjugate acid forms of basic quinuclidine.

Table 1. The pK_a values of the conjugate acids of basic quinuclidine tertiary amine part in cinchona catalysts [a].

Entry	Catalyst[b]	pK_a	Entry	Catalyst[b]	pK_a
1	**HQ**	9.10	7	**HQ-SQ**	7.86
2	**Q**	8.52	8	**Q-SQ**	6.95
3	**DQ**	7.40	9	**DQ-SQ**	6.13
4	**HQ-N**	9.71	10	**HQ-TU**	8.61
5	**Q-N**	9.10	11	**Q-TU**	8.06
6	**DQ-N**	8.10	12	**DQ-TU**	7.02

[a] Conditions: water, 25 °C; [b] The structures are shown in Scheme 1.

2.2. The Effect of the Substituents on Quinuclidine Basicity

Within the four different compound classes (cinchona hydroxyl, amino, thiourea, and squaramide derivatives) the effect of the substituents of quinuclidine on the basicity was examined. As expected,

the saturation of the substituent leads to increased basicity due to electronic reasons. The difference among the pK_a values of the tertiary amino nitrogen in quinuclidine is in a range of 1.6–1.7 in each compound class, depending on the substituents.

2.3. The Effect of the C9 Group of Cinchona on Quinuclidine Basicity

Not only the aliphatic substituent of quinuclidine unit has an effect on the basicity, but the groups of C9 position of the cinchona as well, since these groups and the aliphatic substituents are practically equidistant from the quinuclidine nitrogen. The decreasing order in basicity is the following: amino, hydroxyl, thiourea, and squaramide. This may be caused mainly by electronic effects. Thiourea derivatives have higher basicity than that of the corresponding squaramides. This may be explained by the squaramide moiety having aromatic feature, therefore the electron-withdrawing effect of the bis(trifluoromethyl)phenyl group can have a stronger effect than in the case of thiourea.

2.4. Relationship Between pK_a Values and H-Bonding Abilities

Based on our published results [28–30] and the relevant literature [31,32], in asymmetric Michael additions of 1,3-dioxo compounds to β-nitroalkenes-cinchona, squaramides or thioureas are recommended to be used as enantioselective organocatalysts. Owing to their H-bonding ability (quantified by their pK_a values) [33–38] and chiral skeleton, they not only give high yields but excellent enantioselectivities as well. Despite the fact that the N atom of the quinuclidine ring in thioureas is more basic, the observed enantiomeric excesses are similar than those given by squaramides. This observation can be explained by the different strength of H-bonds formed by thioureas and squaramides.

According to the mechanisms [12–14], cinchona thiourea or squaramide can fix substrates by three H-bonds, while hydroxyl or amino derivatives are able to interact different ways, for instance with less H-bonds. This causes the notable differences among the enantioselectivities. The strong H-bonds can be explained by the relatively high acidity of these units. The pK_a values of thiourea and squaramide units measured in water can be seen in Table 2 (in other solvents see Tables S4 and S5).

Table 2. The pK_a values of acidic squaramide or thiourea units measured in water.

Entry	Catalyst	p$K_{a,\,NH1}$	p$K_{a,\,NH2}$
1	**HQ-SQ**	9.57	11.73
2	**Q-SQ**	9.29	>12 [#]
3	**DQ-SQ**	9.20	>12 [#]
4	**HQ-TU**	10.87	≫12 [#]
5	**Q-TU**	10.84	≫12 [#]
6	**DQ-TU**	10.78	≫12 [#]

[#] nonmeasurable by UV-spectrophotometric titration method.

Based on pK_a values, squaramides are more acidic than thioureas, hence stronger H-bonds can be formed between this moiety and the corresponding substrate. Taking into account the bifunctionality of cinchona thioureas and squaramides, they possess similar catalytic activity: while the quinuclidine nitrogen of cinchona thioureas are more basic, squaramides acidic NH moiety can form stronger H-bonds with the substrate.

Reflecting to further importance of the acidity of the H-bond donor units, an analogue of squaramides, the thiosquaramides having more acidic NH groups should be mentioned [30,38–42]. Thiosquaramides perform better results (yield and ee) in asymmetric Michael addition than the corresponding squaramides. Thiosquaramides could act as Brønsted acids, too. Therefore, they can also catalyze aza-Diels–Alder reaction [30,42], in which neither thioureas nor squaramides can give the desired product.

2.5. Synthesis of the Catalysts

We synthesized the cinchona catalysts starting from the commercially available quinine (**Q**), which was transformed to hydroquinine (**HQ**) by catalytic hydrogenation (Scheme 1). Didehydroquinine (**DQ**) was prepared in a two-step reaction from quinine: a bromine addition was followed by HBr elimination [43].

Cinchona amino derivatives (**HQ-N**, **Q-N**, **DQ-N**) were prepared starting from the relevant hydroxy derivatives (**HQ**, **Q**, **DQ**) based on previously reported procedures [44]. In the next step, thiourea derivatives (**HQ-TU**, **Q-TU**, **DQ-TU**) were obtained by the addition of the appropriate amine derivatives to bis(trifluoromethyl)phenyl isothiocyanate (**SCN**) [45,46]. Finally, addition of the abovementioned amines to half-squaramide methyl ester (**HSQ**) resulted in the corresponding squaramides (**HQ-SQ**, **Q-SQ**, **DQ-SQ**) [46,47]. During the synthetic procedures, all compounds were characterized by well-established methods including MS, IR, ^{1}H, and ^{13}C NMR spectroscopies.

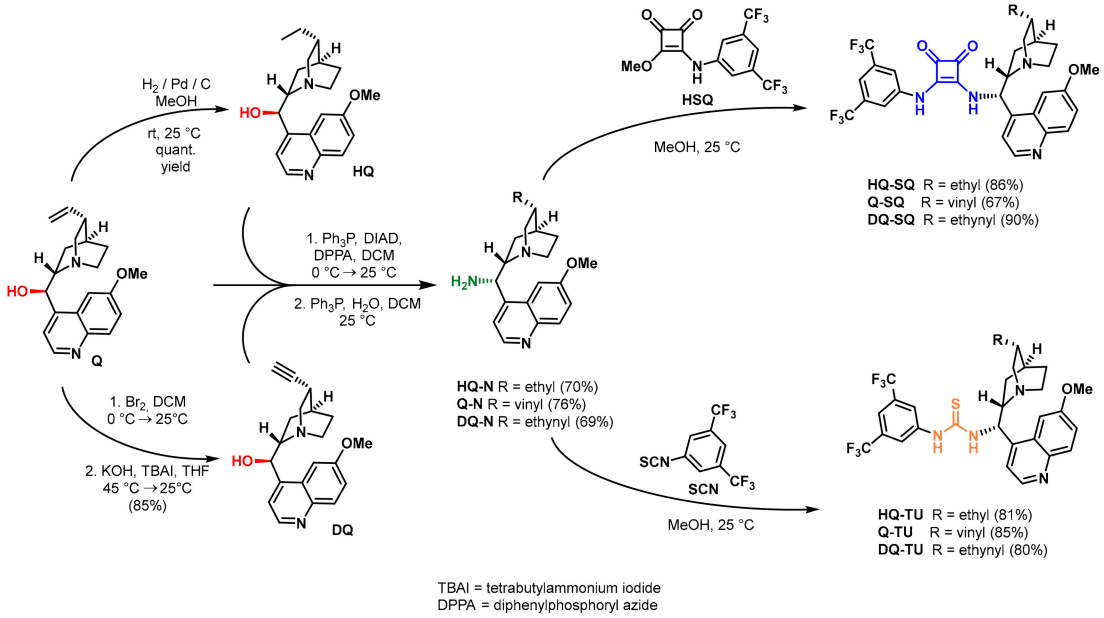

Scheme 1. The synthesis of cinchona-based organocatalysts.

2.6. Application of the Catalysts in Asymmetric Michael Addition

We used hydroxy, amine, thiourea, and squaramide type catalysts in Michael addition (Scheme 2) of pentane-2,4-dione (**2**) to *trans*-β-nitrostyrene (**1**). Conventional and green solvents including dichloromethane (DCM), methyl *tert*-butyl ether (MTBE), toluene, acetonitrile (MeCN), ethyl acetate (EtOAc), methanol, and tetrahydrofuran (THF) were used (Table 3 and Table S5) under the same conditions. In methanol, which is a protic solvent, we got only lower yields (up to 82% vs. up to 100%) and enantioselectivities (up to 51% ee vs. up to 93% ee). This observation is in agreement with similar cinchona-based organocatalysis [48]. In methanol, hydrogen bonds could form between the solvent and the catalysts/reactants. Accordingly, to apply a hydrogen bonding organocatalyst in protic polar solvents, could result in low yields and enantiomeric excesses.

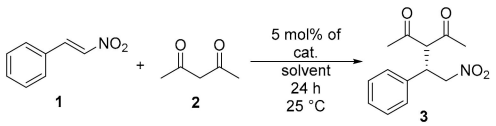

Scheme 2. Michael Addition of pentane-2,4-dione (**2**) to trans-β-nitrostyrene (**1**).

Table 3. Catalysts applied in Michael addition using *trans*-β-nitrostyrene (**1**) and pentane-2,4-dione (**2**) [a].

Entry	Catalyst	Solvent	Yield [%][b]	ee [%][c]
1	**HQ-SQ**	DCM	99	85
2	**HQ-SQ**	MTBE	100	75
3	**HQ-SQ**	toluene	100	82
4	**HQ-SQ**	MeCN	97	84
5	**HQ-SQ**	EtOAc	99	81
6	**HQ-SQ**	MeOH	77	45
7	**HQ-SQ**	THF	99	85
8	**Q-SQ**	DCM	98	87
9	**Q-SQ**	MTBE	99	90
10	**Q-SQ**	toluene	99	89
11	**Q-SQ**	MeCN	99	86
12	**Q-SQ**	EtOAc	100	89
13	**Q-SQ**	MeOH	76	51
14	**Q-SQ**	THF	99	81
15	**DQ-SQ**	DCM	99	89
16	**DQ-SQ**	MTBE	76	82
17	**DQ-SQ**	toluene	87	90
18	**DQ-SQ**	MeCN	88	80
19	**DQ-SQ**	EtOAc	89	83
20	**DQ-SQ**	MeOH	76	38
21	**DQ-SQ**	THF	95	70
22	**HQ-TU**	DCM	93	87
23	**HQ-TU**	MTBE	99	91
24	**HQ- TU**	toluene	95	90
25	**HQ- TU**	MeCN	94	84
26	**HQ- TU**	EtOAc	99	86
27	**HQ- TU**	MeOH	76	25
28	**HQ- TU**	THF	97	78
29	**Q- TU**	DCM	100	85
30	**Q- TU**	MTBE	99	89
31	**Q- TU**	toluene	100	91
32	**Q- TU**	MeCN	99	78
33	**Q- TU**	EtOAc	100	85
34	**Q- TU**	MeOH	82	25
35	**Q- TU**	THF	99	82
36	**DQ- TU**	DCM	98	91
37	**DQ- TU**	MTBE	97	66
38	**DQ- TU**	toluene	99	93
39	**DQ- TU**	MeCN	85	73
40	**DQ- TU**	EtOAc	80	86
41	**DQ- TU**	MeOH	76	17
42	**DQ- TU**	THF	98	90

Michael adducts were obtained in high yields (up to 99%) when hydroxyl or amino derivatives of cinchona were applied, but these reactions gave only 34% ee (see Table S5). Concerning selectivity, no significant difference was found between the differently saturated cinchonas; however, among hydroxy derivatives in most of the solvents, **HQ** gave higher enantiomeric excesses. It can be explained by its higher basicity, but this tendency cannot be observed in cases of other derivatives.

The utilization of squaramides or thioureas served both high yields (up to 100%, see Table 3) and enantioselectivities (up to 93% ee, see Table 3 and Figure 3). The different pK_a values of these derivatives did not lead to significant changes in yield or enantiomeric excess. Squaramides and thioureas gave good results in asymmetric Michael addition, without showing any considerable difference in the catalytic activity.

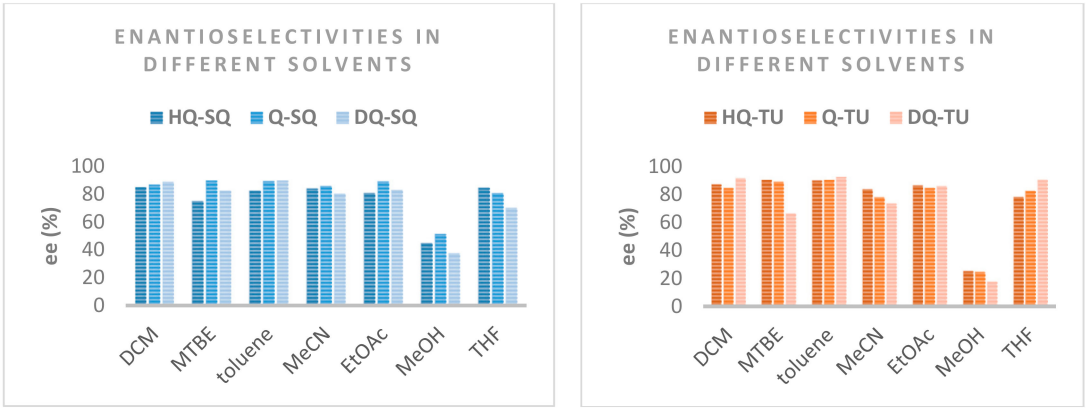

(**a**) (**b**)

[a] Reaction conditions: pentane-2,4-dione (**2**) (0.41 mmol) was added to the solution of *trans*-β-nitrostyrene (**1**) (0.16 mmol) and 5 mol% catalysts in 1 mL of solvent, then the resulting mixture was stirred at room temperature for 24 h; [b] Isolated yield; [c] Determined by chiral HPLC (*S* enantiomer).

Figure 3. Enantioselectivities given in different solvents when squaramides (**a**) or thioureas (**b**) were applied in Michael addition.

2.7. Theoretical Calculations

Due to the importance of hydrogen bonds and acidity in the catalytic mechanisms of cinchona-thiourea compounds [49,50], one of the main questions is how the ethyl, ethynyl, and vinyl substituents can affect their acid-base properties. Therefore, we investigated systematically the different tautomers of the synthesized **HQ-TU**, **Q-TU**, and **DQ-TU** catalysts and their protonated and deprotonated forms using quantum chemical calculations.

In agreement with their similar reactivities observed in the experiments, the geometric structures of the neutral cinchona and thiourea frameworks (see Figures S22 and S23 in the Supplementary Materials) and also the energetics of the different tautomers, as well as the protonation and deprotonation Gibbs free energies (Figure 4 and Figures S22 and S23, Table 4 and Table S6 in the Supplementary Materials) depend only slightly on the ethyl, ethynyl, or vinyl substituents. In all cases, the most stable tautomer is the thione form, containing two NH groups (*i* on Figure 4), while the quinuclidine nitrogen is protonated in the higher-lying tautomers *ii* and *iii*. Interestingly, in the higher-lying isomers the proton detaches from the bis(trifluoromethyl)phenyl side of the thiosquaramide. We expect that this is due to the interaction with the nitrogen lone pair with the π system, leading to an increased acidity at this site.

The thiol form *iv* is lying even higher in free energy. Thus, overall the calculations show that among the possible tautomers the catalytically most active [49,50] *i* is the most stable form and present in considerably higher amount than the others.

Electrostatic potential provides important insights into the intermolecular interactions of similar compounds [51,52]. The electrostatic potentials (see the Supplementary Materials, Figure S24) clearly show that both the sulfur and the nitrogen atoms are possible protonation sites. The calculations showed that in line with the above discussion, the quinuclidine nitrogen is the preferred site in all cases, with proton affinity of ~−44 kJ·mol^{-1} (Figure 4). The protonated thiol form of the cinchona-thiourea lies about 62 kJ·mol^{-1} higher in free energy, while the proton affinity decreases to −14 kJ·mol^{-1}. Thus, the computations show that the quinuclidine is the main protonation site in acidic conditions.

Interestingly, in contrary to the neutral tautomers, there is only 9–12 kJ·mol^{-1} difference between the two possible deprotonated forms, indicating that both of the possible tautomers present in acidic conditions.

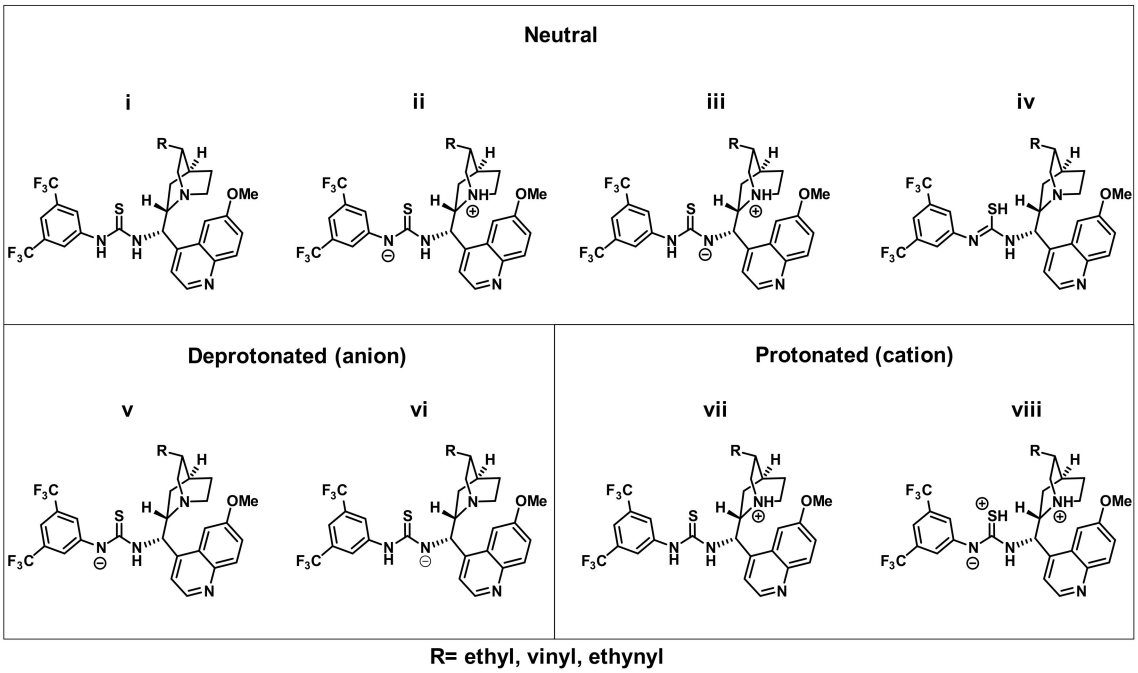

Figure 4. The significant neutral, deprotonated, and protonated tautomer forms of thioureas.

Table 4. Relative Gibbs free energies (kJ·mol^{-1}) of the energetically lowest-lying tautomers of thioureas (HQ-TU, Q-TU, DQ-TU) and their deprotonated anion and protonated cation forms in THF.

Compound	Neutral				Deprotonated (anion)		Protonated (cation)	
	i	ii	iii	iv	v	vi	vii	viii
HQ-TU	0	32	59	64	0 (150)	9 (159)	0 (−44)	62 (−14)
Q-TU	0	32	63	65	0 (148)	10 (157)	0 (−46)	69 (−9)
DQ-TU	0	40	66	70	0 (144)	12 (157)	0 (−40)	64 (−9)

Protonation and deprotonation Gibbs free energies of the corresponding neutral tautomer are indicated in parentheses. (ωB97X-D/6-311++G**+SM12// ωB97X-D/6-31G*+SM8 method; see Figure 4 for notation).

3. Conclusions

In conclusion, we can approach bifunctional H-bond organocatalysts in two ways: focusing on their H-bond acceptor or donor abilities (Figure 5).

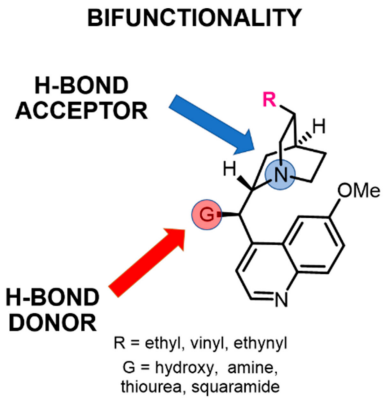

Figure 5. The bifunctional sites of the represented cinchona organocatalysts.

As H-bond acceptors: within each compound class (hydroxyl, amino, squaramide, thiourea) the bifunctional cinchona organocatalysts with differently saturated substituents on basic quinuclidine

nitrogen have 1.6–1.7 difference in their pK_a values. The strongest bases are the compounds substituted with ethyl, followed by vinyl and then ethynyl groups. No significant difference was found in yields and enantioselectivities in any compound classes applying them in Michael addition. The basicity in each compound class increases in the following order: amino, hydroxyl, squaramides, thiourea.

As H-bond donors: the catalysts, which are able to form dual H-bonds gave the highest enantiomeric excesses (thioureas and squaramides). The squaramides have by 1.3–1.6 lower pK_a values than the corresponding thioureas, resulting in stronger H-bonds with the substrate.

By summarizing the H-bond abilities, cinchona thioureas are better acceptors, but as donors, squaramides show stronger interactions. As organocatalysts in Michael addition, there is no considerable difference among them, both the yields and enantiomeric excesses were similar in each solvent and, within these compounds, the saturation had no effect on yield and ee as well.

Based on our results, saturation of the substituent at the quinuclidine unit has no significant effect on the catalysis thus the most easily available quinine derivatives (vinyl substituent at quinuclidine) are worth to apply as cinchona-based organocatalysts as themselves or as starting materials of their C9 derivatives. Considering immobilization, vinyl is a suitable group for further modifications, for instance in polymerization, or forming a reactive group in the molecule for this purpose.

Our results were corroborated by computational studies. Accordingly, the saturation of the substituent on quinuclidine has a slight effect on basicity of the H-bond acceptor nitrogen atom. Moreover, we accomplished calculations on stability of different tautomer forms of thiourea catalysts. These calculations approved that the most stable tautomers in all cases are the thione forms with the proton residing on the nitrogen atom of the quinuclidine.

4. Experimental

The UV/pH titrations were performed using D-PAS technique (Dip-Probe Absorbance Spectrophotometry, a quartz fiber dip probe measuring absorbance using a flow-cell) attached to a SiriusT3 instrument (Pion Inc., Forest Row, UK) [53,54]. The pK_a values were calculated by SiriusT3Refine™ software (Pion Inc., Forest Row, UK). All measurements were performed in solutions of 0.15M KCl under nitrogen atmosphere, at t = 25.0 ± 0.1 °C. The cosolvent dissociation constants (p$_s K_a$ values) of the compounds were also determined in various MeOH–water mixtures between 15 and 70 wt% and MeCN–water, dioxane–water, THF–water, DMSO–water mixtures between 15 and 50 wt%. Each sample was measured at least in minimum six different cosolvent–water ratios. To obtain the 98.0% and 99.9% cosolvent p$_s K_a$ values from p$_s K_a$ data, linear and Yasuda–Shedlovsky extrapolation methods have been used. The Yasuda–Shedlovsky method establishes a correlation with the dielectric constant and uses the following equation: p$_s K_a$ + log[H_2O] = $a\ \varepsilon + b$, where log[H_2O] is the molar water concentration of the given solvent mixture. This method is the most widely used procedure in cosolvent techniques [55,56].

Infrared spectra were recorded on a Bruker Alpha-T FT-IR spectrometer (Bruker, Ettlingen, Germany). Optical rotations were measured on a Perkin-Elmer 241 polarimeter (Perkin-Elmer, Waltham, MA, USA) that was calibrated by measuring the optical rotations of both enantiomers of menthol. NMR spectra were recorded at Directorate of Drug Substance Development, Egis Pharmaceuticals Plc., on a Bruker Avance III HD (Bruker, Ettlingen, Germany) (at 600 MHz for ^{1}H and at 150 MHz for ^{13}C spectra). Mass spectra were recorded on CAMAG LCMS Interface (CAMAG, Muttenz, Switzerland) (HPLC pump: Shimadzu LC-20AD Prominence SQ MS: Shimadzu LCMS-2020 MS settings: detector voltage: 1.10 kV, *m/z*: 105–1000, scan speed: 1075 u·s^{-1}, DL temperature: 250 °C, nebulizing gas flow: 1.5 L·min^{-1}, drying gas flow: 15 L·min^{-1}, eluent: acetonitrile: 0.1% (*v/v*) formic acid 95:5, 1.5 mL·min^{-1}). The exact mass measurements were performed using Q-TOF Premier mass spectrometer (Waters Corporation, 34 Maple St, Milford, MA, USA) in positive electrospray ionization mode. The enantiomeric ratios of the samples were determined by chiral high-performance liquid chromatography (HPLC) measurements using reversed-phase mode (Thermo Finnigan Surveyor LC System, Thermo Fisher Scientific, Waltham, MA, USA). Elemental analyses were performed in the

Microanalytical Laboratory of the Department of Organic Chemistry, Institute for Chemistry, Eötvös Loránd University, Budapest, Hungary. Melting points were taken on a Boetius micro-melting point apparatus (VEB Dresden Analytik, Dresden, Germany) and they were uncorrected. Starting materials were purchased from Aldrich Chemical Company (St. Louis, MO, USA) unless otherwise noted. Silica gel 60 F_{254} (Merck, Darmstadt, Germany) plates and aluminium oxide 60 F_{254} (Merck) were used for TLC. The spots of materials on TLC plates were visualized by UV light at 254 nm. Silica gel 60 (70–230 mesh, Merck) was used for column chromatography. Ratios of solvents for the eluents are given in milliliters.

The lowest energy tautomers were obtained using the MMFF94 force, as it is implemented in the Avogadro program [57]. Subsequently, the geometry optimization of the neutral structures as well as of their protonated and deprotonated forms were carried out using Density Functional Theory applying the ωB97X-D functional [58] and 6-31G* basis set [59], as it is implemented in the Q-Chem 5.2 quantum chemical software package [60], while the final energy computations were performed using the 6-311++G** basis set. The applied density functional includes long range and dispersion corrections and the accuracy of this method has been tested for similar systems in our previous studies [28–30]. The (75,302) integration grid was applied in all cases. The geometries of the catalysts were optimized both in the gas phase and in THF solvent using SM8 [61] and the SS(V)PE [62]. Harmonic vibrational frequencies were computed in the gas phase for the most stable tautomers. These show no imaginary vibrational frequencies, confirming that the computed conformers are minima on the potential energy surface. Single-point calculations were carried out using the SM12 solvent model [63]. As it is expected, the different solvent models yield similar results for the relative energies of the different structures (the maximum absolute deviation is 14 kJ mol^{-1}, see Table S6 in the Supplementary Materials) and similar accuracy is obtained for protonation free energies (the maximum absolute error is 13 kJ mol^{-1}), however much larger differences are obtained for anions (maximum error in deprotonation free energies is 47 kJ mol^{-1}). Nevertheless, both solvent models yield the same tendencies. During the computation of the relative Gibbs free energies, the vibrational contribution is neglected and only the solvation contribution is considered. For the protonation and deprotonation computation, the solvation Gibbs free energy of the proton in THF is necessary, however, its computation is a tedious task. We approximated this quantity using a supermolecule model consisting of a proton and two THF molecules, embedded in a continuum solvent [64]. The molecules were visualized using the PyMol program [65].

4.1. Hydroquinine

A solution of quinine (2.00 g, 6.17 mmol) in methanol (20 mL) was added to a suspension of Pd/C in methanol (20 mL) under argon atmosphere. The quinine was hydrogenated at 25 °C under atmospheric pressure. When the reaction was completed (1 h), the reaction mixture was filtered through a pad of Celite. The solvent was evaporated, giving pure hydroquinine (**HQ**, Figure 6) as a white solid (2.01 g, 99%). Spectral data are fully consistent with those reported in the literature [66].

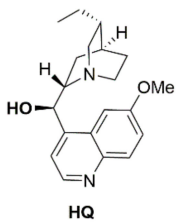

HQ

Figure 6. Structure of **HQ**.

4.2. (S)-((1S,2S,4S,5S)-5-Ethynylquinuclidin-2-yl)(6-methoxyquinolin-4-yl)methanamine

Triphenylphosphine (976 mg, 3.72 mmol) was added to a solution of **DQ** (1.00 g, 3.10 mmol) in DCM (6 mL) under argon atmosphere and stirred for 1 h at room temperature. The reaction mixture

was cooled down to 0 °C and a solution of DIAD (740 µL, 753 mg, 3.72 mmol) in DCM (1 mL) was added to it dropwise. After addition, the reaction mixture was stirred at room temperature overnight. Then the reaction mixture was cooled down to 0 °C, and water (1.35 mL, 75 mmol) was added to it in one portion. After this step, a solution of triphenylphosphine (1.46 g, 5.58 mmol) in DCM (5 mL) was added dropwise to the reaction mixture and it was stirred overnight at 25 °C. After the reaction was completed, the mixture was diluted to 50 mL with DCM, and it was shaken with an aqueous hydrochloric acid solution (2 × 50 mL, 10 w%). The combined inorganic phase was cooled down to 0 °C, and its pH was adjusted to 10 with aqueous sodium hydroxide solution and extracted with DCM (2 × 50 mL). The combined organic phase was dried over $MgSO_4$, and the solvent was evaporated under reduced pressure. Further purification was not necessary. The product is a brownish-yellow, viscous oil (**DQ-N**, Figure 7, 673 mg, 69%). TLC (SiO_2 TLC; DCM:MeOH:25% NH_4OH = 10:1:0.01, R_f = 0.52; $[a]_{20}^{D}$ + 86.7 (c 1.00, $CHCl_3$); IR ν_{max} 3424, 3294, 2930, 2862, 1621, 1589, 1508, 1474, 1454, 1431, 1356, 1620, 1260, 1229, 1028 cm^{-1}; ^1H NMR (600 MHz, DMSO-d_6, 25 °C): δ (ppm) 0.76 (1 H, m), 1.35 (1 H, m), 1.41 (1 H, m), 1.49 (1 H, m), 1.67 (1 H, bm), 2.51 (1 H, m), 2.62 (1 H, m), 2.79 (1 H, m), 2.83 (1 H, m), 3.07 (1 H, bm), 3.22 (1 H, bm), 3.32 (1 H, m), 3.94 (3 H, s), 4.64 (1 H, bm), 7.42 (1 H, dd, $J_{1,H,H}$ 2.8 Hz, $J_{2,H,H}$ 9.2 Hz), 7.59 (1 H, bm), 7.80 (1 H, bm), 7.95 (1 H, d, $J_{H,H}$ 9.2 Hz), 8.72 (1 H, d, $J_{H,H}$ 4.5 Hz); ^{13}C NMR (150 MHz, DMSO-d_6, 25 °C): δ (ppm) 25.9, 26.0, 26.7, 26.9, 55.7, 57.2, 61.5, 71.2, 79.4, 88.5, 102.9, 120.5, 121.4, 128.7, 129.0, 131.4, 144.3, 147.9 (2 C), 157.1; HRMS-ESI+ *m/z* [M + H^+] calcd. for $C_{20}H_{24}N_3O$: 322.1919, found: 322.1923.

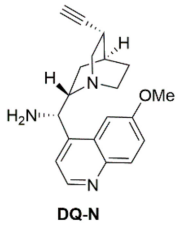

Figure 7. Structure of **DQ-N**.

4.3. 3-((3,5-Bis(trifluoromethyl)phenyl)amino)-4-(((S)-((1S,2S,4S,5R)-5-ethynylquinuclidin-2-yl)(6-methoxyquinolin-4-yl)methyl)amino)cyclobut-3-ene-1,2-dione

A solution of **DQ-N** (Figure 7) (200 mg, 0.67 mmol) in chloroform (0.7 mL) was added to a solution of half squaramide (**HSQ**: 322 mg, 0.74 mmol) in chloroform (1.5 mL). This mixture was stirred for 12 h at room temperature. The solvent was removed under reduced pressure, then the crude product was purified by column chromatography on silica gel using DCM: methanol:25% NH_4OH (10:1:0.01) mixture as an eluent to obtain the pure product as white crystals (**DQ-SQ**, Figure 8, 387 mg, 99%). M.p. 240 °C (decomposes). TLC (SiO_2 TLC; DCM:MeOH:25% NH_4OH = 10:1:0.01, R_f = 0.52; $[a]_{20}^{D}$ −104.8 (c 1.00, $CHCl_3$); IR ν_{max} 3441, 3315, 3213, 2934, 1796, 1669, 1623, 1573, 1512, 1455, 1380, 1279, 1186, 1129, 1042 cm^{-1}; ^1H NMR (600 MHz, DMSO-d_6, 25 °C): δ (ppm) 0.76 (1 H, bm), 1.45 (1 H, bm), 1.55 (1 H, bm), 1.65 (1 H, bm), 1.77 (1 H, bm), 2.60 (1 H, m), 2.88 (1 H, m), 2.96 (1 H, bm), 3.28 (1 H, m), 3.34 (1 H, m), 3.57 (1 H, bm), 3.97 (3 H, s), 6.11 (1 H, bm), 7.48 (1 H, dd, $J_{1,H,H}$ 2.3 Hz, $J_{2,H,H}$ 9.1 Hz), 7.62 (1 H, d, $J_{H,H}$ 4.0 Hz), 7.67 (1 H, bm), 7.76 (1 H, bm), 7.97 (2 H, m), 8.01 (1 H, d, $J_{H,H}$ 9.1 Hz), 8.39 (1 H, bm), 8.86 (1 H, d, $J_{H,H}$ 4.0 Hz), 10.15 (1 H, bs); ^{13}C NMR (150 MHz, DMSO-d_6, 25 °C): δ (ppm) 25.7, 26.3, 26.7 (2 C), 55.1, 55.9, 57.0, 59.0, 71.5, 88.3, 101.6, 115.2, 118.6, 119.3, 122.2, 123.3 (q, $J_{C,F}$ 273 Hz), 127.7, 128.9, 129.0, 131.4 ($J_{C,F}$ 33 Hz), 131.8, 141.0, 143.2, 144.5, 148.0, 158.0, 162.9, 168.8, 180.4, 185.1; HRMS-ESI+ *m/z* [M+H^+] calcd. for $C_{32}H_{27}N_4O_3F_6$: 629.1987, found: 629.1990.

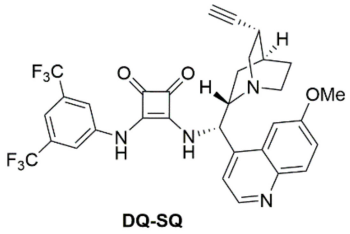

Figure 8. Structure of DQ-SQ.

*4.4. General Procedure for Michael Addition of Pentane-2,4-dione (**2**) to Trans-β-nitrostyrene (**1**).*

To a solution of *trans*-β-nitrostyrene (**1**) (23.4 mg, 0.16 mmol) in the corresponding solvent (1 mL), organocatalyst (5 mol%) was added. Then, pentane-2,4-dione (**2**) (41.5 µL, 40.7 mg, 0.41 mmol) was added to this solution and the resulting reaction mixture was stirred at room temperature. After 24 h, the volatile components were removed under reduced pressure. The crude product was purified by preparative thin-layer chromatography on silica gel using hexane:ethyl acetate 2:1 mixture (R_f = 0.36) as eluent to obtain Michael adduct (*S*)-**3** as white crystals. Yields and enantiomeric excess (ee) values can be seen in in the Table 3 and Table S5. Spectral data are fully consistent with those reported in the literature (the absolute configuration was determined by the optical rotation of the products) [28]. HPLC: Phenomonex Lux Cellulose-3 column (3 mm, 250 × 4.6 mm), eluent CH_3CN/20 mM NH_4OAc in H_2O = 40/60, isocratic mode; 0.6 mL min^{-1}; UV detector 222 nm, 5 µL or 10 µL injection, 20 °C. Retention time for (*S*)-**3**: 11.94 min, for (*R*)-**3**: 14.20 min.

Supplementary Materials: Supplementary data to this article can be found online at http://www.mdpi.com/1996-1944/12/18/3034/s1. These data include solvent screening of asymmetric Michael additions, FT-IR spectra, characterization of ^1H, ^{13}C and 2D NMR spectra and MS spectra of new products, furthermore, the chiral HPLC profiles, the pK_a measurements, and theoretical calculations.

Author Contributions: Methodology, S.N., P.K., and J.K.; synthesis of compounds, S.N. and Z.F.; performing pK_a measurements, data analysis, Gergő Dargó and G.T.B.; performing quantum-chemical studies, conducting discussion of the results, J.B. and T.H.; performing NMR experiments, data analysis, Z.G.; determination of ee values by chiral HPLC measurements, B.M.; writing—original draft preparation, S.N. and J.B.; writing—review and editing, J.K., T.H., P.H., G.T.B., P.K., Z.F., and Gyula Dargó; project administration, J.K.; funding acquisition, P.H. and J.K.; resources, P.H. and J.K.; supervision, J.K.

Funding: This research was funded by the New National Excellence Program of the Ministry of Human Capacities, grant numbers ÚNKP-18-4-BME-270 and ÚNKP-18-2-II-BME-243, and the János Bolyai Research Scholarship of the Hungarian Academy of Science. It was also supported by the National Research, Development, and Innovation Office (grant number K128473), the Servier–Beregi PhD Research Fellowship, and the Gedeon Richter's Talentum Foundation.

Acknowledgments: The authors are grateful to Joanna Kacperek and Magdalena Potępa from Lodz University of Technology, International Faculty of Engineering, for their assistance with the synthetic work, to László Drahos from MS Proteomics Research Group, Research Centre for Natural Sciences, Hungarian Academy of Sciences, for his assistance with the HRMS measurements, and to András Dancsó from Egis Pharmaceuticals Plc., Directorate of Drug Substance Development, for his assistance with the NMR measurements.

Conflicts of Interest: The authors declare no conflict of interest.

References

1. Nag, A.; Gergelitsová, I.; Veselý, J.; Adly, F.G.; Ghanem, A.; Moriuchi, T.; Ohmura, S.D.; Hirao, T.; McCluskey, A.; Simone, M.I.; et al. *Asymmetric Synthesis of Drugs and Natural Products*, 1st ed.; CRC Press: Boca Raton, FL, USA, 2019; pp. 1–485.
2. Houk, K.N.; List, B. Asymmetric organocatalysis. *Acc. Chem. Res.* **2004**, *37*, 487. [CrossRef]
3. MacMillan, D.W.C. The advent and development of organocatalysis. *Nature* **2008**, *455*, 304–308. [CrossRef] [PubMed]
4. Zhan, G.; Du, W.; Chen, Y.C. Switchable divergent asymmetric synthesis via organocatalysis. *Chem. Soc. Rev.* **2017**, *46*, 1675–1692. [CrossRef] [PubMed]

5. Hughes, D.L. Biocatalysis in Drug Development-Highlights of the Recent Patent Literature. *Org. Proc. Res. Dev.* **2018**, *22*, 1063–1080. [CrossRef]
6. Connon, S.J. Asymmetric catalysis with bifunctional cinchona alkaloid-based urea and thiourea organocatalysts. *Chem. Commun. (Camb.)* **2008**, *22*, 2499–2510. [CrossRef] [PubMed]
7. Yoon, T.P.; Jacobsen, E.N. Privileged chiral catalysts. *Science* **2003**, *299*, 1691–1693. [CrossRef] [PubMed]
8. Yeboah, E.M.O.; Yeboah, S.O.; Singh, G.S. Recent applications of Cinchona alkaloids and their derivatives as catalysts in metal-free asymmetric synthesis. *Tetrahedron* **2011**, *67*, 1725–1762. [CrossRef]
9. Kato, K.; Zhang, M.R.; Suzuki, K. Synthesis of (R,S)-[4-C-11]baclofen via Michael addition of nitromethane labeled with short-lived C-11. *Bioorg. Med. Chem. Lett.* **2009**, *19*, 6222–6224. [CrossRef]
10. Hajzer, V.; Fisera, R.; Latika, A.; Durmis, J.; Kollar, J.; Frecer, V.; Tucekova, Z.; Miertus, S.; Kostolansky, F.; Vareckova, E.; et al. Stereoisomers of oseltamivir—Synthesis, in silico prediction and biological evaluation. *Org. Biomol. Chem.* **2017**, *15*, 1828–1841. [CrossRef]
11. Jung, J.C.; Park, O.S. Efficient asymmetric synthesis of prostaglandin E-1. *Z Naturforsch B* **2007**, *62*, 556–560. [CrossRef]
12. Okino, T.; Hoashi, Y.; Furukawa, T.; Xu, X.N.; Takemoto, Y. Enantio- and diastereoselective Michael reaction of 1,3-dicarbonyl compounds to nitroolefins catalyzed by a bifunctional thiourea. *J. Am. Chem. Soc.* **2005**, *127*, 119–125. [CrossRef] [PubMed]
13. Hamza, A.; Schubert, G.; Soos, T.; Papai, I. Theoretical studies on the bifunctionality of chiral thiourea-based organocatalysts: Competing routes to C-C bond formation. *J. Am. Chem. Soc.* **2006**, *128*, 13151–13160. [CrossRef] [PubMed]
14. Kotai, B.; Kardos, G.; Hamza, A.; Farkas, V.; Papai, I.; Soos, T. On the Mechanism of Bifunctional Squaramide-Catalyzed Organocatalytic Michael Addition: A Protonated Catalyst as an Oxyanion Hole. *Chem. Eur. J.* **2014**, *20*, 5631–5639. [CrossRef] [PubMed]
15. Varga, E.; Mika, L.T.; Csampai, A.; Holczbauer, T.; Kardos, G.; Soos, T. Mechanistic investigations of a bifunctional squaramide organocatalyst in asymmetric Michael reaction and observation of stereoselective retro-Michael reaction. *RSC Adv.* **2015**, *5*, 95079–95086. [CrossRef]
16. Grayson, M.N. Mechanism and Origins of Stereoselectivity in the Cinchona Thiourea- and Squaramide-Catalyzed Asymmetric Michael Addition of Nitroalkanes to Enones. *J. Org. Chem.* **2017**, *82*, 4396–4401. [CrossRef] [PubMed]
17. Porta, R.; Benaglia, M.; Coccia, F.; Cozzi, F.; Puglisi, A. Solid Supported 9-Amino-9-deoxy-epi-quinine as Efficient Organocatalyst for Stereoselective Reactions in Batch and Under Continuous Flow Conditions. *Adv. Synth. Catal.* **2015**, *357*, 377–383. [CrossRef]
18. Kacprzak, K.M.; Maier, N.M.; Lindner, W. Highly efficient immobilization of Cinchona alkaloid derivatives to silica gel via click chemistry. *Tetrahedron Lett.* **2006**, *47*, 8721–8726. [CrossRef]
19. Lee, J.W.; Mayer-Gall, T.; Opwis, K.; Song, C.E.; Gutmann, J.S.; List, B. Organotextile Catalysis. *Science* **2013**, *341*, 1225–1229. [CrossRef]
20. Parvez, M.M.; Haraguchi, N.; Itsuno, S. Synthesis of Cinchona Alkaloid-Derived Chiral Polymers by Mizoroki-Heck Polymerization and Their Application to Asymmetric Catalysis. *Macromolecules* **2014**, *47*, 1922–1928. [CrossRef]
21. Kohout, M.; Wernisch, S.; Tuma, J.; Hettegger, H.; Picha, J.; Lindner, W. Effect of different immobilization strategies on chiral recognition properties of Cinchona-based anion exchangers. *J. Sep. Sci.* **2018**, *41*, 1355–1364. [CrossRef]
22. Fredriksen, K.A.; Kristensen, T.E.; Hansen, T. Combined bead polymerization and Cinchona organocatalyst immobilization by thiol-ene addition. *Beilstein J. Org. Chem.* **2012**, *8*, 1126–1133. [CrossRef] [PubMed]
23. Song, C.E.; Blaser, H.-U.; Ager, D.J.; Deshmukh, R.R.; Ryu, D.H.; Shin, U.S.; Lee, J.E.; Yang, J.W.; Park, H.-G.; Jeong, B.-S.; et al. *Cinchona Alkaloids in Synthesis and Catalysis*, 1st ed.; Wiley-VCH Verlag GmbH & Co. KGaA: Weinheim, Germany, 2009; pp. 1–506.
24. Kumpuga, B.T.; Itsuno, S. Synthesis of Crosslinked Chiral Polysiloxanes of Cinchona Alkaloid Derivatives and their Applications in Asymmetric Catalysis. *Asian J. Org. Chem.* **2019**, *8*, 251–256. [CrossRef]
25. Etzenbach-Effers, K.; Berkessel, A. Noncovalent Organocatalysis Based on Hydrogen Bonding: Elucidation of Reaction Paths by Computational Methods. *Top. Curr. Chem.* **2009**, *291*, 1–27.

26. Knowles, R.R.; Jacobsen, E.N. Attractive noncovalent interactions in asymmetric catalysis: Links between enzymes and small molecule catalysts. *Proc. Natl. Acad. Sci. USA* **2010**, *107*, 20678–20685. [CrossRef] [PubMed]
27. Doyle, A.G.; Jacobsen, E.N. Small-molecule H-bond donors in asymmetric catalysis. *Chem. Rev.* **2007**, *107*, 5713–5743. [CrossRef] [PubMed]
28. Didaskalou, C.; Kupai, J.; Cseri, L.; Barabas, J.; Vass, E.; Holtzl, T.; Szekely, G. Membrane-Grafted Asymmetric Organocatalyst for an Integrated Synthesis-Separation Platform. *ACS Catal.* **2018**, *8*, 7430–7438. [CrossRef]
29. Kisszekelyi, P.; Alammar, A.; Kupai, J.; Huszthy, P.; Barabas, J.; Holtzl, T.; Szente, L.; Bawn, C.; Adams, R.; Szekely, G. Asymmetric synthesis with cinchona-decorated cyclodextrin in a continuous-flow membrane reactor. *J. Catal.* **2019**, *371*, 255–261. [CrossRef]
30. Nagy, S.; Dargo, G.; Kisszekelyi, P.; Feher, Z.; Simon, A.; Barabas, J.; Holtzl, T.; Matravolgyi, B.; Karpati, L.; Drahos, L.; et al. New enantiopure binaphthyl-cinchona thiosquaramides: Synthesis and application for enantioselective organocatalysis. *New J. Chem.* **2019**, *43*, 5948–5959. [CrossRef]
31. Vakulya, B.; Varga, S.; Csampai, A.; Soos, T. Highly enantioselective conjugate addition of nitromethane to chalcones using bifunctional cinchona organocatalysts. *Org. Lett.* **2005**, *7*, 1967–1969. [CrossRef]
32. Malerich, J.P.; Hagihara, K.; Rawal, V.H. Chiral Squaramide Derivatives are Excellent Hydrogen Bond Donor Catalysts. *J. Am. Chem. Soc.* **2008**, *130*, 14416–14417. [CrossRef]
33. Jakab, G.; Tancon, C.; Zhang, Z.G.; Lippert, K.M.; Schreiner, P.R. (Thio)urea Organocatalyst Equilibrium Acidities in DMSO. *Org. Lett.* **2012**, *14*, 1724–1727. [CrossRef] [PubMed]
34. Ni, X.; Li, X.; Cheng, J.P. Equilibrium acidities of cinchona alkaloid organocatalysts bearing 6′-hydrogen bonding donors in DMSO. *Org. Chem. Front.* **2016**, *3*, 170–176. [CrossRef]
35. Ni, X.; Li, X.; Wang, Z.; Cheng, J.P. Squaramide Equilibrium Acidities in DMSO. *Org. Lett.* **2014**, *16*, 1786–1789. [CrossRef] [PubMed]
36. Xue, X.S.; Yang, C.; Li, X.; Cheng, J.P. Computational Study on the pK(a) Shifts in Proline Induced by Hydrogen-Bond-Donating Cocatalysts. *J. Org. Chem.* **2014**, *79*, 1166–1173. [CrossRef] [PubMed]
37. Zwicker, V.E.; Yuen, K.K.Y.; Smith, D.G.; Ho, J.M.; Qin, L.; Turner, P.; Jolliffe, K.A. Deltamides and Croconamides: Expanding the Range of Dual H-bond Donors for Selective Anion Recognition. *Chem. Eur. J.* **2018**, *24*, 1140–1150. [CrossRef]
38. Ho, J.M.; Zwicker, V.E.; Yuen, K.K.Y.; Jolliffe, K.A. Quantum Chemical Prediction of Equilibrium Acidities of Ureas, Deltamides, Squaramides, and Croconamides. *J. Org. Chem.* **2017**, *82*, 10732–10736. [CrossRef] [PubMed]
39. Busschaert, N.; Elmes, R.B.P.; Czech, D.D.; Wu, X.; Kirby, I.L.; Peck, E.M.; Hendzel, K.D.; Shaw, S.K.; Chan, B.; Smith, B.D.; et al. Thiosquaramides: pH switchable anion transporters. *Chem. Sci.* **2014**, *5*, 3617–3626. [CrossRef]
40. Lu, T.X.; Wheeler, S.E. Origin of the Superior Performance of (Thio)Squaramides over (Thio)Ureas in Organocatalysis. *Chem. Eur. J.* **2013**, *19*, 15141–15147. [CrossRef]
41. Rombola, M.; Sumaria, C.S.; Montgomery, T.D.; Rawal, V.H. Development of Chiral, Bifunctional Thiosquaramides: Enantioselective Michael Additions of Barbituric Acids to Nitroalkenes. *J. Am. Chem. Soc.* **2017**, *139*, 5297–5300. [CrossRef]
42. Rombola, M.; Rawal, V.H. Dicyclopentyl Dithiosquarate as an Intermediate for the Synthesis of Thiosquaramides. *Org. Lett.* **2018**, *20*, 514–517. [CrossRef]
43. Braje, W.M.; Frackenpohl, J.; Schrake, O.; Wartchow, R.; Beil, W.; Hoffmann, H.M.R. Synthesis of 10,11-didehydro Cinchona alkaloids and key derivatives. *Helv. Chim. Acta* **2000**, *83*, 777–792. [CrossRef]
44. McCooey, S.H.; Connon, S.J. Readily accessible 9-epi-amino cinchona alkaloid derivatives promote efficient, highly enantioselective additions of aldehydes and ketones to nitroolefins. *Org. Lett.* **2007**, *9*, 599–602. [CrossRef] [PubMed]
45. Vakulya, B.; Varga, S.; Soos, T. Epi-cinchona based thiourea organocatalyst family as an efficient asymmetric Michael addition promoter: Enantioselective conjugate addition of nitroalkanes to chalcones and alpha,beta-unsaturated N-acylpyrroles. *J. Org. Chem.* **2008**, *73*, 3475–3480. [CrossRef] [PubMed]
46. del Pozo, S.; Vera, S.; Oiarbide, M.; Palomo, C. Catalytic Asymmetric Synthesis of Quaternary Barbituric Acids. *J. Am. Chem. Soc.* **2017**, *139*, 15308–15311. [CrossRef] [PubMed]

47. Bae, H.Y.; Some, S.; Lee, J.H.; Kim, J.Y.; Song, M.J.; Lee, S.; Zhang, Y.J.; Song, C.E. Organocatalytic Enantioselective Michael-Addition of Malonic Acid Half-Thioesters to beta-Nitroolefins: From Mimicry of Polyketide Synthases to Scalable Synthesis of gamma-Amino Acids. *Adv. Synth. Catal.* **2011**, *353*, 3196–3202. [CrossRef]
48. Grosseheilmann, J.; Kragl, U. Simple and Effective Catalyst Separation by New CO2-Induced Switchable Organocatalysts. *ChemSusChem* **2017**, *10*, 2685–2691. [CrossRef]
49. Madarasz, A.; Dosa, Z.; Varga, S.; Soos, T.; Csampai, A.; Papai, I. Thiourea Derivatives as Bronsted Acid Organocatalysts. *ACS Catal.* **2016**, *6*, 4379–4387. [CrossRef]
50. Hammar, P.; Marcelli, T.; Hiemstra, H.; Himo, F. Density functional theory study of the Cinchona thiourea-catalyzed henry reaction: Mechanism and enantioselectivity. *Adv. Synth. Catal.* **2007**, *349*, 2537–2548. [CrossRef]
51. Quinonero, D.; Frontera, A.; Suner, G.A.; Morey, J.; Costa, A.; Ballester, P.; Deya, P.M. Squaramide as a binding unit in molecular recognition. *Chem. Phys. Lett.* **2000**, *326*, 247–254. [CrossRef]
52. Quinonero, D.; Prohens, R.; Garau, C.; Frontera, A.; Ballester, P.; Costa, A.; Deya, P.M. A theoretical study of aromaticity in squaramide complexes with anions. *Chem. Phys. Lett.* **2002**, *351*, 115–120. [CrossRef]
53. Allen, R.I.; Box, K.J.; Comer, J.E.; Peake, C.; Tam, K.Y. Multiwavelength spectrophotometric determination of acid dissociation constants of ionizable drugs. *J. Pharm. Biomed. Anal.* **1998**, *17*, 699–712. [CrossRef]
54. Tam, K.Y.; Takacs-Novak, K. Multi-wavelength spectrophotometric determination of acid dissociation constants: A validation study. *Anal. Chim. Acta* **2001**, *434*, 157–167. [CrossRef]
55. Avdeef, A.; Comer, J.E.A.; Thomson, S.J. Ph-Metric Log. 3. Glass-Electrode Calibration in Methanol Water, Applied to Pka Determination of Water-Insoluble Substances. *Anal. Chem.* **1993**, *65*, 42–49. [CrossRef]
56. TakacsNovak, K.; Box, K.J.; Avdeef, A. Potentiometric pK(a) determination of water-insoluble compounds: Validation study in methanol/water mixtures. *Int. J. Pharm.* **1997**, *151*, 235–248. [CrossRef]
57. Hanwell, M.D.; Curtis, D.E.; Lonie, D.C.; Vandermeersch, T.; Zurek, E.; Hutchison, G.R. Avogadro: An advanced semantic chemical editor, visualization, and analysis platform. *J. Cheminform.* **2012**, *4*, 17. [CrossRef]
58. Chai, J.D.; Head-Gordon, M. Long-range corrected hybrid density functionals with damped atom-atom dispersion corrections. *Phys. Chem. Chem. Phys.* **2008**, *10*, 6615–6620. [CrossRef] [PubMed]
59. Hariharan, P.C.; Pople, J.A. The influence of polarization functions on molecular orbital hydrogenation energies. *Theor. Chim. Acta* **1973**, *28*, 213–222. [CrossRef]
60. Shao, Y.H.; Gan, Z.T.; Epifanovsky, E.; Gilbert, A.T.B.; Wormit, M.; Kussmann, J.; Lange, A.W.; Behn, A.; Deng, J.; Feng, X.T.; et al. Advances in molecular quantum chemistry contained in the Q-Chem 4 program package. *Mol. Phys.* **2015**, *113*, 184–215. [CrossRef]
61. Cramer, C.J.; Truhlar, D.G. A universal approach to solvation modeling. *Acc. Chem. Res.* **2008**, *41*, 760–768. [CrossRef]
62. Chipman, D.M.; Dupuis, M. Implementation of solvent reaction fields for electronic structure. *Theor. Chem. Acc.* **2002**, *107*, 90–102. [CrossRef]
63. Marenich, A.V.; Cramer, C.J.; Truhlar, D.G. Generalized Born Solvation Model SM12. *J. Chem. Theory Comput.* **2013**, *9*, 609–620. [CrossRef] [PubMed]
64. Zhan, C.G.; Dixon, D.A. Absolute hydration free energy of the proton from first-principles electronic structure calculations. *J. Phys. Chem. A* **2001**, *105*, 11534–11540. [CrossRef]
65. *The PyMOL Molecular Graphics System, V.S.*; LLC Schrodinger: New York, NY, USA, 2010.
66. Palacio, C.; Connon, S.J. A New Class of Urea-Substituted Cinchona Alkaloids Promote Highly Enantioselective Nitroaldol reactions of Trifluoromethylketones. *Org. Lett.* **2011**, *13*, 1298–1301. [CrossRef] [PubMed]